Available online at www.sciencedirect.com

ScienceDirect

Procedia Materials Science 9 (2015) 538 – 547

Procedia Materials Science

www.elsevier.com/locate/procedia

International Congress of Science and Technology of Metallurgy and Materials, SAM – CONAMET 2014

Fretting damage in Incoloy® 800 tubes against different support materials

S.R.Soria[a,c,]*, J.P. Balbiani[a], M. Bergant[b], A. Tolley[a,c], A. Yawny[a,c]

[a]*División Física de Metales, Centro Atómico Bariloche - Instituto Balseiro, CNEA - Av. E. Bustillo 9500, 8400 S. C. de Bariloche, Argentina.*
[b]*Gerencia CAREM, Centro Atómico Bariloche, CNEA - Av. E. Bustillo 9500, 8400 S.C. de Bariloche, Argentina.*
[c]*CONICET (Consejo Nacional de Investigaciones Científicas y Técnicas).*

Abstract

In this work the fretting wear in steam generator tubes of Incoloy® 800 in contact with AISI 304, AISI 1060 and Cu (99,9 %) pads acting in a cross-tube geometry was studied. Wear surface was characterized by scanning electron microscopy (SEM) and the resulting debris were characterized by transmission electron microscopy (TEM) and energy dispersive spectroscopy (EDS). It was verified that in all cases, the fretting conditions corresponded to gross slip. A predominance of adhesive wear was found for Cu and AISI 1060 while abrasive wear was predominant in the case of AISI 304. It was determined that the higher the hardness of the pad material the lower the surface damage (case of the AISI 1060). Analysis of debris allowed the identification non-stoichiometric oxide phases with either a spinel structure of the type $FeCr_2O_4.Fe_3O_4$ and a hematite $(Fe,Cr)_2O_3$ in the case of AISI 304, while for Cu and AISI 1060 pads, the presence of $CuFe_2O_4$ spinel and $(Fe,Cr)_2O_3$ hematite were observed, respectively. The formation of spinel structures originates in an effect of mechanical alloying between the surfaces. Debris particle size distribution was found to extend in the range from tens of nanometers to few micrometers with the larger particles consisting in agglomerates of crystallites with sizes between 5 and 20 nm.

Peer-review under responsibility of the Scientific Committee of SAM–CONAMET 2014

*Keywords:*800, fretting wear, SEM, TEM

* Corresponding author. Tel.: +54-294-4445304; fax: +54-294-4445299.
E-mail address: sergio.soria@ib.edu.ar

Peer-review under responsibility of the Scientific Committee of SAM–CONAMET 2014
doi:10.1016/j.mspro.2015.05.027

1. Introduction

Fretting is a type of wear damage induced in two surfaces in contact under a relative movement of small amplitude (1 to 300 µm) and involves different mechanisms such as abrasion, adhesion and tribochemical reactions, among others [Waterhouse (1972)]. The nature and chemical composition of materials in contact [Bethune and Waterhouse (1968), Blanchard et al. (1991)] and surface hardness [Budinski (2013)] have been reported as factors with important effects in the wear process.

In steam generator tubes (SGTs) in nuclear reactors, fretting is one of principal mechanisms responsible of tube degradation. Flow induced vibration (FIV) is the origin of the phenomena [Fisher et al. (1995)] provoking the relative movement between the tubes and their supporting plates.

In the Pressurized Water Reactors (PWRs), a material often used in the fabrication of SGTs is the alloy 800 also known as Incoloy®800 [Special Metals (2004)]. This is a Fe-Ni superalloy and has been used in SGTs due to its excellent corrosion resistance and adequate mechanical properties at working temperatures around 300 ºC. Most of investigations on this material were carried out under conditions favoring fretting wear using different load and environment conditions and configurations of cross-tubes [Hong and Kim (2003)] or plate-tube [Guérout and Fisher (1995)]. However, the effects of different materials involved in the contact pair have not received so much attention so far.

In the present work, fretting wear of SGTs in contact with pads of different materials was studied. The characteristics of the surface damage (scars) and the structure of the debris generated during the fretting process have been investigated using Scanning Electron Microscopy (SEM) and Transmission Electron Microscopy (TEM).

2. Material and methods

Incoloy®800 tubes (I 800) with a diameter of 15.87 mm and wall thickness of 1.13 mm were used. The support plate was simulated with stainless steel AISI 304, carbon steel AISI 1060 and Cu semi-cylindrical pads with a radius of 6.35 mm. The contact geometry used was that of 90º cross-tubes, resulting in a point contact. The nominal composition (in weight percentage) of the different materials considered along the present work is shown in Table 1.

Table 1. Chemical nominal composition (wt %) of the different materials used in the present work.

Material	Fe	Ni	Cr	Cu	C	Mn	S	Si
I 800 [Special Metals (2004)]	39.5 min.	30-35	19-23	0.75 max.	0.1 max.	1.5 max.	0.15 max.	1 max.
AISI 304 [ASM International (1985)]	66.6 min.	8-10	18-20	-	0.08 max.	2 max.	0.03 max.	0.75 max.
AISI 1060 [ASM International (1990)]	98 min.	-	-	-	0.55-0.65	0.6-0.9	0.05 max.	0.15-0.35
Cu	-	-	-	99.9	-	-	-	-

Fretting tests were realized in a MTS 810 servo-hydraulic testing machine using a device which is schematically illustrated in Fig. 1. The normal load between the SGT and the pad was applied using an elastic cantilever beam supported from the upper grip of the testing machine. The SGT was supported on the lower grip which was moved by the piston. All tests were carried out in air (temperature 25 ºC, relative humidity 35%) at a frequency of 15 Hz using constant normal load $F = 40 \pm 2$ N and a displacement amplitude $\delta = 75 \pm 5$ µm up to 1E6 cycles. In this way, the consequence of using different material pairs, under the mentioned conditions, was assessed.

Surface damage (scars) was characterized by Scanning Electron Microscopy (SEM) using a Philips 515 SEM. The scars were studied at end of the test and after cleaning the specimen surface in an ultrasonic bath. On the other hand, debris generated during tests was dissolved in ethanol to obtain a colloidal suspension. A Cu grid with Formvar/Carbon film was submerged in the suspension to support the particles for TEM analysis. Microstructural characterization of debris was carried out with a 200 kV Philips CM200 TEM equipped with an Ultratwin lens. The local elemental composition in the different regions of the scars and debris was determined by Energy Dispersive X-ray Spectroscopy (EDS) performed in SEM and TEM, respectively.

Finally, the Vickers hardness (HV) of the tube and pads was determined using a Mitutoyo MKV-H0 using a load of 0.5 kg applied for 20 seconds.

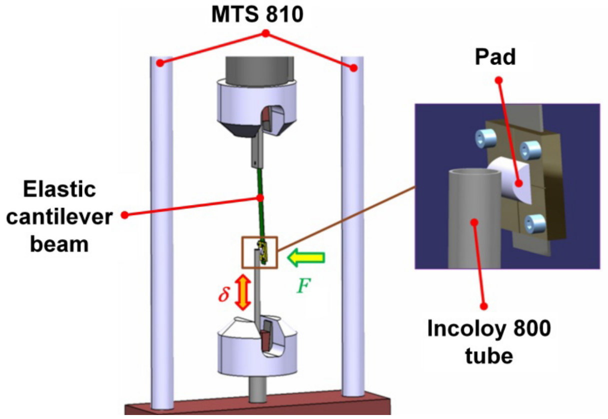

Fig. 1. Schematic of the fretting wear test rig.

3. Results and discussion

In all cases, scars in both surfaces presented a circular shape due to the 90° cross cylinder geometry used. The software ImageJ 1.46 [Rasband (2014)] was employed in the determination of geometric parameters of the scars such as area (A), perimeter (P) and diameter Feret (dF). Using Eqs. (1)-(2) the average diameter (D) and shape factor (SF) can be obtained conform to ASTM standards [Hetzner (2008)]. The results are shown in Table 2.

$$D = \frac{4 \cdot A}{P} \tag{1}$$

$$SF = \frac{4 \cdot A}{\pi \cdot dF^2} \tag{2}$$

Table 2. Average diameter (D) and shape factor (SF) of scars for the different materials pairs.

Pair of Materials	D [mm]		SF [dimensionless].	
	SGT	Pad	SGT	Pad
I 800/Cu	4.311	4.27	0.977	0.906
I 800/AISI 304	4.306	4.51	0.969	0.917
I 800/AISI 1060	3.901	4.35	0.906	0.881

In every test, the SGT-pad system was in gross slip regime where the relative displacement takes place in all the surface in contact with sliding wear marks appearing in the fretting direction [Vingsbo and Söderberg (1988)].

Based on the results of Table 2, the most uniform wear between both surfaces was obtained in the case of the I 800/Cu pair where the scars in both surfaces have similar values of D. Wear in the SGT was the smallest in the I 800/AISI 1060 pair.

Comparing SF values of Table 2, it can be seen that some scars were more elliptical than others (SF = 1 for a circumference). This could be understood considering a rolling effect of the pads over the SGT. The presence of a friction force in the contact area between surfaces and the distance between the contact region and neutral fiber of the elastic cantilever beam providing the normal load applied generated a corresponding alternative bending moment. This caused the rolling between pads and SGTs that lead the scar to adopt an elliptical shape [Briscoe et al. (1998)]. The relative importance of rolling over tangential displacement will depend on the magnitude of the friction force. The effect was verified to be greater in the case of the I 800/AISI 1060 pair.

The characteristics of the scars were different for every pair of materials. In case of the I 800/Cu pair, the principal effects of fretting wear can be appreciated in Fig. 2. It can be seen that wear was predominantly adhesive as shown in Fig. 2(a), with the formation of a compact debris layer on the SGT surface, as shown in Fig. 2(b). In the pad surface, material loss by delamination took place as illustrated in Fig. 2(c). On the other hand, Fig. 2(d) shows that material transfer occurred between surfaces in contact.

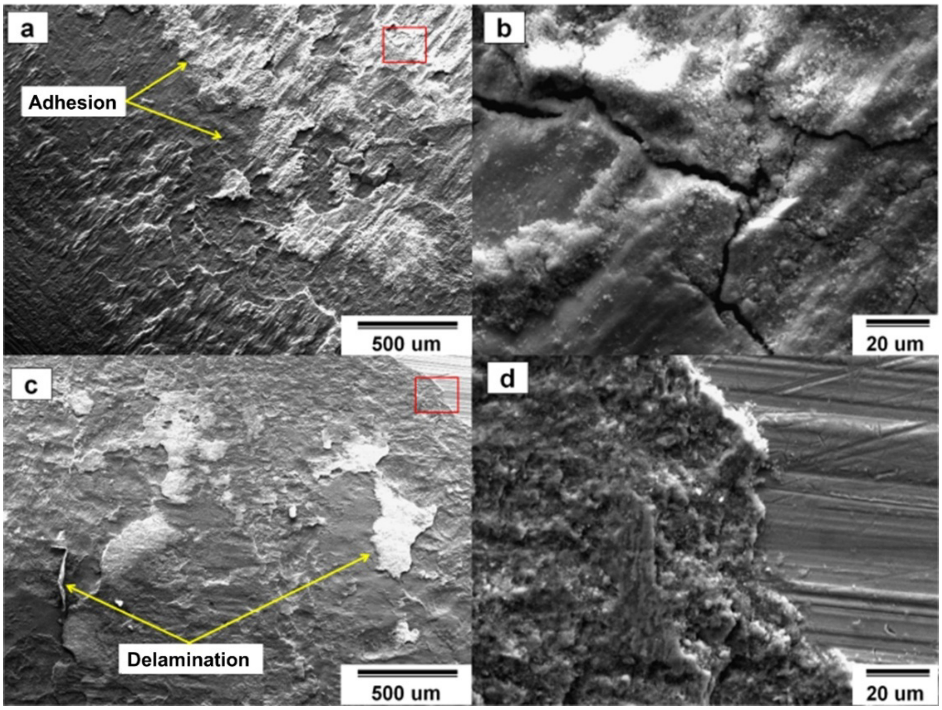

Fig. 2. Surface damage by fretting wear in pair I 800 (SGT) /Cu (pad) on SGT (a, b) and pad (c, d).

A change in wear mode was found for the I 800/AISI 304 pair. In this case, a predominance of abrasive wear compared to adhesive wear was detected. In addition, the generation of grooves and microcutting in the contact area are visible from Fig. 3(c) while a small amount of adhesion over the surfaces of the pad and the SGT can be seen from Figs. 3(a)-(d). The formation of a compact debris layer with a weak adherence is shown in Fig. 3 (b) where the layer has been detached after cleaning the specimen in an ultrasonic bath,

In case of the I 800/AISI 1060 pair, the main wear mechanism observed was adhesive wear, as shown in Fig. 4(a). Here, a small degree of abrasion on the surface, resulting in the formation of grooves is observed in Fig. 4(b). On the pad surface, Fig. 5, material transfer between surfaces was verified through the formation of two debris layers presenting different contrast. EDS analysis of the darker layer in region (a) determined that debris presented a similar composition to that of the pad, with a higher concentration of Fe. Instead, analysis of the layer in region (b) suggests that it corresponds to debris of the SGT having higher concentration of Fe, Cr and Ni.

Table 3 presents the results of Vickers Hardness (HV) for the different materials used. In Fig. 6, the dependence of scar size in SGT expressed in terms of average diameter is presented. It can be seen that an increase in pad hardness results in a reduction of scar size, i.e. in a diminution of fretting damage in the SGTs. This is in line with previous results reported in the literature [Budinski (2013)] where it has been found that similar hardness values of SGTs and pads resulted in a reduction of damage by fretting wear.

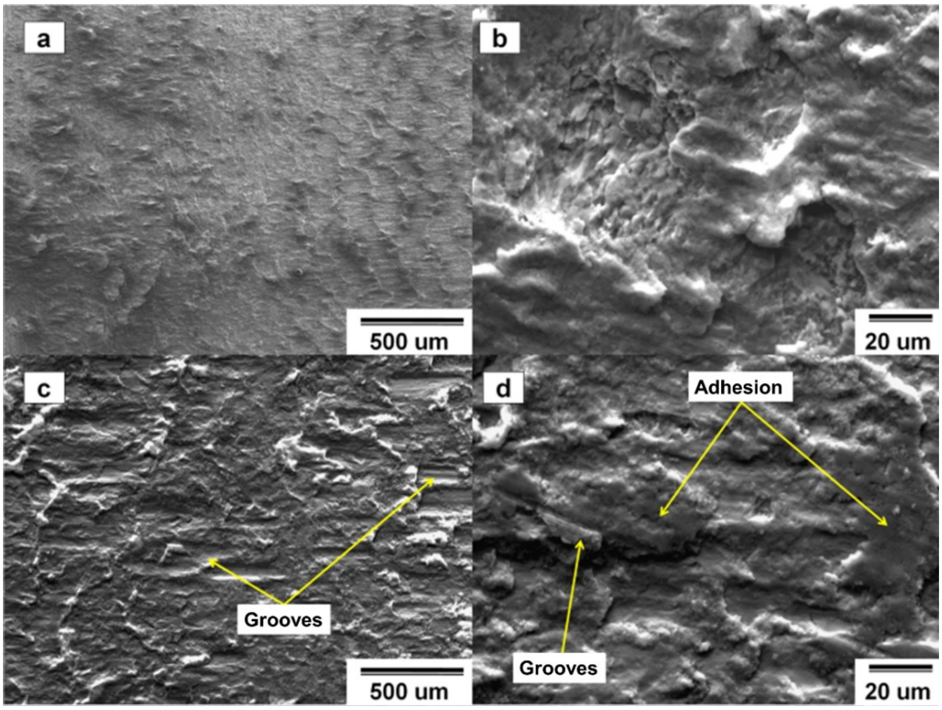

Fig. 3. Surface damage by fretting wear in pair I 800 (SGT)/AISI 304 (pad) on SGT (a, b) and pad (c, d).

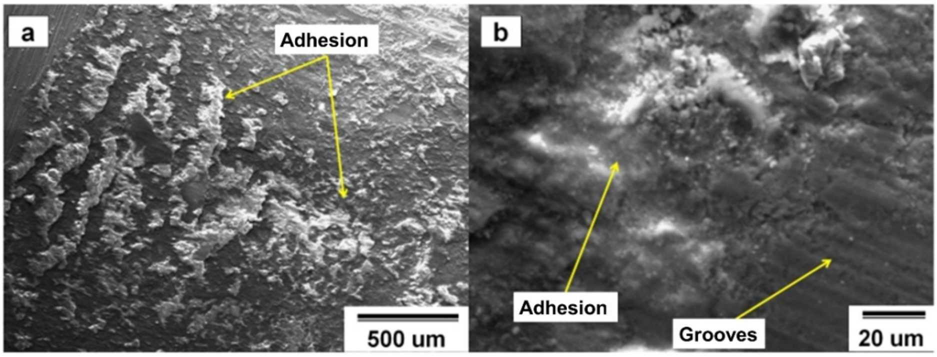

Fig. 4. Surface damage by fretting wear in pair I 800 (SGT)/AISI 1060 (pad) on SGT (a) and pad (b).

Using TEM analysis it was found that the debris particle size distribution varies from tens of nanometers to a few micrometers, as can be seen in Fig. 7. Using High Resolution TEM (HRTEM) it was determined that the larger particles were formed by agglomeration of small crystallites sized between 5 to 20 nm as shown in Fig. 8.

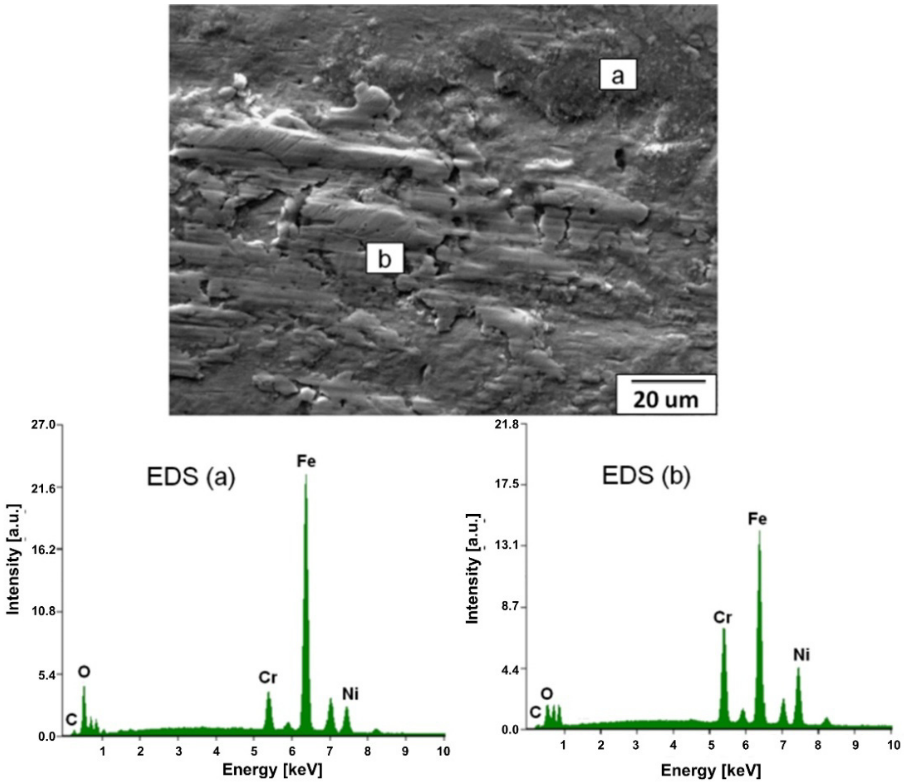

Fig 5. Debris on pad in the pair I 800 (SGT)/AISI 1060 (pad) with similar composition to pad (a) and SGT (b).

Table 3. Vickers Hardness (HV) of the different materials used.

Material	I 800	Cu	AISI 304	AISI 1060
HV	215±22	143±7	321±23	753±43

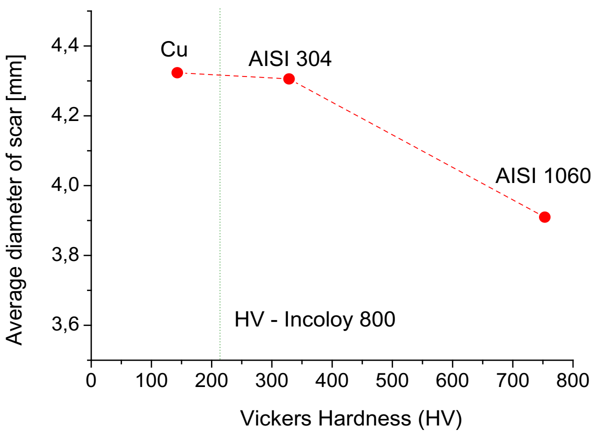

Fig. 6. Size scar on SGT as a function of pad hardness.

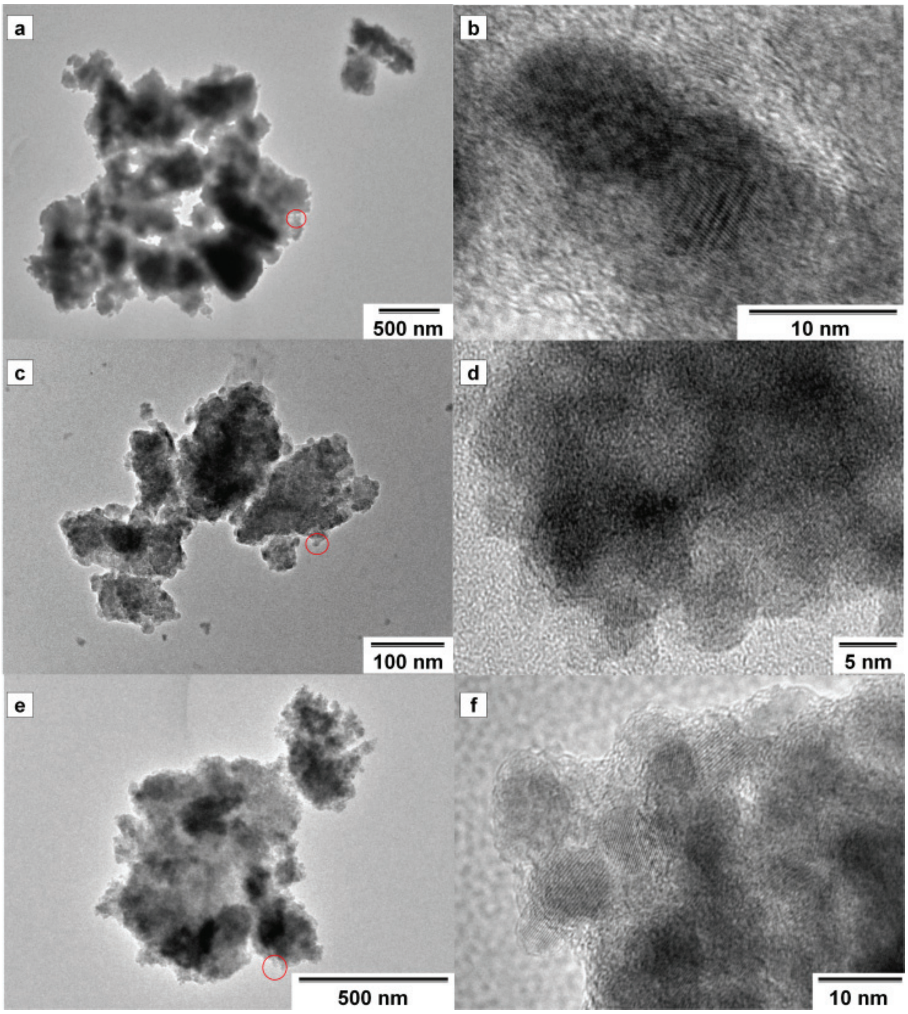

Fig. 7. TEM micrographs of debris for different pairs of materials: I 800 (SGT)/Cu (pad) (a, b), I 800 (SGT)/AISI 304 (pad) (c, d) and I 800 (SGT)/AISI 1060 (pad) (e, f).

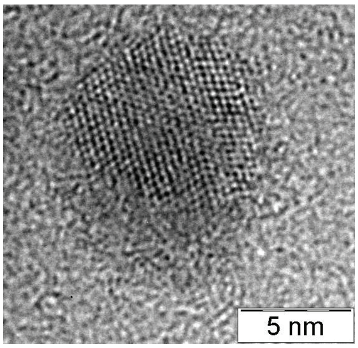

Fig. 8. Nano-sized debris of 5 nm of the pair I 800 (SGT)/AISI 304 (pad).

Electron diffraction patterns were employed to determine the structure of debris, as shown in Fig. 9. Debris particles, with sizes between 100 and 200 nm, were analyzed.

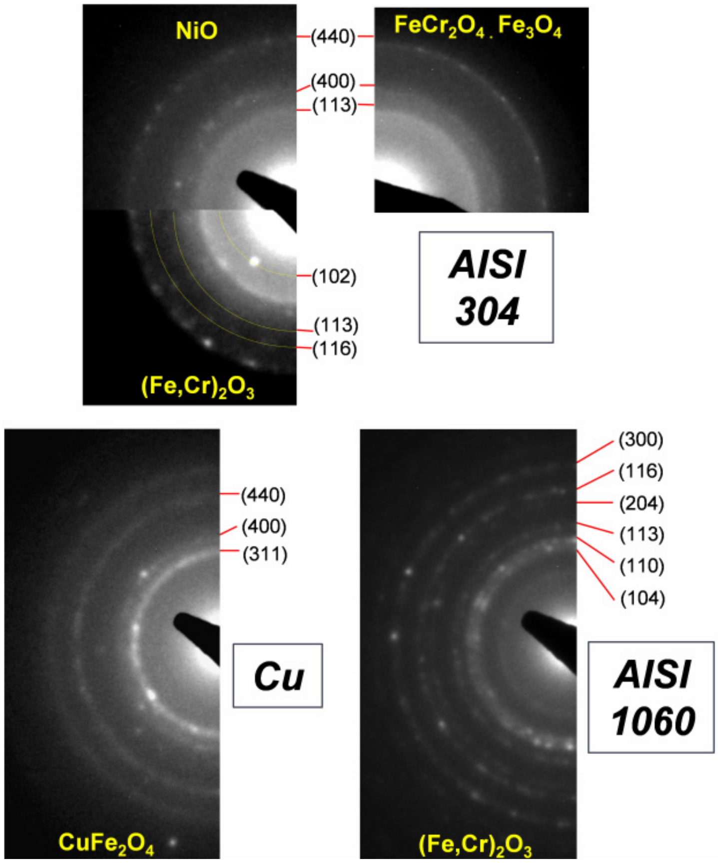

Fig. 9. Diffraction patterns from debris particles formed by agglomeration of nano-crystallites for the different pad materials.

In case of the I 800/AISI 304 pair, three different oxides were found in the debris: a spinel, a hematite and NiO. EDS analysis performed with a 30 nm diameter electron beam indicated that the oxides were non-stoichiometric in composition since the Fe, Ni and Cr local concentrations were variable in different zones of the same debris. Analysis of the diffraction patterns suggested that the spinel could be formulated as $Fe_3O_4.FeCr_2O_4$ while the hematite could be formulated as $(Fe,Cr)_2O_3$. In these oxides, Fe^{2+} ions occupy tetrahedral sites while Fe^{3+} and Cr^{3+} ions occupy octahedral sites.

In the case of the I 800/Cu and I 800/AISI 1060 pairs debris were single phase. For the Cu pad, a spinel structure was formed that could be formulated as $CuFe_2O_4$. For the AISI 1060 pad, a hematite structure was identified that could be formulated as $(Fe,Cr)_2O_3$, with Fe^{3+} and Cr^{3+}occupying octahedral sites. The Fe-based spinels, also known as ferrites, are usually obtained by high temperature mechanical milling of precursor oxides like Fe_2O_3 and bivalent metal oxide [Cullity and Graham (2009)]. During the fretting wear process, debris are retained between contact surfaces where they suffer a process similar to mechanical milling which is accompanied by a local temperature increase due to friction effects.

The formation of non-stoichiometric oxides of spinel and hematite structures in AISI 304 has been studied in relation with corrosion effects in aqueous environments at temperatures up to 288ºC [Kuang et al. (2010)]. However, the detailed mechanisms for the formation of such structures are not yet completely established. Formation of

$CuFe_2O_4$ cuprospinel has been reported in studies of mechanical alloying of CuO and Fe_2O_3 at temperatures over 800ºC [Marinca et al. (2012)]. This suggests that for the I 800/Cu pair, the formation of cuprospinel can be explained by the presence of these precursor oxides and by the local temperature increase to nearly 800°C due to friction effects.

The change in the dominant wear mechanism from adhesive (Cu and AISI 1060 pads) to abrasive (AISI 304 pad) can be explained in terms of the structures formed during the tests.

In fretting wear, abrasion results from a third-body grinding originated in the presence of triboparticles formed during the process. They are generally oxides and their role can be understood considering the hardness ratio between the oxide particle and the metal matrix [Hurricks (1970)]. A higher hardness ratio indicates that the oxide will have a stronger abrasive character than the matrix. For Fe, the hardness ratio takes values between 3:1 to 10:1 while for Cu and Ni, it takes values of 1:1 to 3:1 [Hurricks (1970)]. Therefore, the expected predominant wear mechanism is abrasion in AISI 304 and AISI 1060 pads. On other hand, in the I 800/AISI 304 pair a protective layer of Cr_2O_3 exists both on the pad and SGT surface, with hardness values reaching 1350 HV [Kitsunai et al. (1991)] while in the I 800/AISI 1060 pair, the high hardness of the pad could help prevent third-body abrasion. Then, the formation of high hardness particles in between the metallic surfaces in contact during the fretting wear process in the I 800/AISI 304 pair seems to determine that the predominant mechanism is abrasive wear.

4. Conclusion

In this work, the fretting wear of Incoloy®800 steam generator tubes in contact with Cu, AISI 304 and AISI 1060 pads was studied. A change in the dominant wear mechanism was found for the different pads. Adhesive wear was predominant for Cu and AISI 1060 pads while for the AISI 304 pad, abrasive wear was dominant. This can be explained based on structures of debris formed during the fretting wear process.

Analysis of scars showed a more homogenous wear in the I 800/Cu pair, while the surface wear was smaller for the I 800/ AISI 1060 pair. In addition, a reduction of surface wear in the tubes with increasing pad hardness was found.

A wide distribution of debris particle sizes was found in all cases, where the larger particles were formed by an agglomeration of crystallites with sizes of 5 to 20 nm. The analysis of these particles showed that for the Cu and AISI 1060 pads debris was of a single phase, a spinel and a hematite respectively, while for the AISI 304 pad three principal phases were found, a spinel, a hematite and a Face-Centered Cubic structure. The increase of abrasive wear in the I 800/AISI 304 pair was due to presence of high hardness phases, for example Cr_2O_3.

Acknowledgements

The authors acknowledge support from the Atomic Energy Commission of Argentina (CNEA) and ANPCyT PICT 0898-2011. Help with SEM imaging by Mr. Carlos Cotaro is gratefully acknowledged.

References

ASM international, 1990. *Metals Handbook Vol. 1: Properties and Selection: Irons, Steels, and High-Performance Alloy*. American Society for Metals, Materials Park, Ohio.

ASM international, 1985. *Metals Handbook Vol.9: Metallography and Microstructure*. American Society for Metals, Metals Park, Ohio.

Bethune, B., Waterhouse, R.B., 1968.Adhesion of metal surfaces under fretting conditions II. Unlike metals in contact. Wear 12, 369.

Blanchard, P., Colombie, C.,Pellerin, V.,Fayeulle, S., Vincent, L., 1991.Material Effects in Fretting Wear: Application to Iron, Titanium and Aluminum Alloys. Metallurgical TransactionsA 22, 1535.

Briscoe, B.J., Chateauminois, A., Lindley, T.C., Parsonage,D., 1998. Fretting wear behaviour ofpolymethylmethacrylate underlinear motions and torsionalcontact conditions. Tribology International 31, 701.

Budinski,K.G., 2013. Effect of hardness differential on metal-to-metal fretting damage. Wear 301, 501.

Cullity, B.D., Graham, C.D., 2009.*Introduction to magnetic materials*. Willey, New Jersey.

Fisher, N.J., Chow, A.B.,Weckwerth, M.K., 1995.Experimental Fretting-Wear Studies of Steam Generator Materials. Journal of Pressure Vessel Technology ASME 117, 312.

Guérout, F. M., Fisher, N. J., 1995. SteamGeneratorFretting-Wear Damage:ASummaryofRecentFindings. Journal Pressure Vessel Technology 121, 304.

Hetzner, D.W., 2008. Comparing Binary Image Analysis Measurements - Euclidean Geometry, Centroids and Corners. Microscopy Today 16, 10.

Hong, J.K., Kim, I.S., 2003.Environment effects on the reciprocating wearof Inconel 690 steam generator tubes. Wear 255, 1174.

Hurricks, P. L., 1970. The mechanics of fretting – A review.Wear 15, 389.

Kitsunai, H., Hokkirigawa, K., Tsumaki, N., Kato, K., 1991. Transitions of microscopic wear mechanism for Cr_2O_3 ceramic coatings during repeated sliding observed in a scanning electron microscope tribosystem. Wear 151, 279.

Kuang, W., Han, E.H., Wu, X., Rao, J., 2010. Microstructural characteristics of the oxide scale formed on 304 stainless steelin oxygenated high temperature water. Corrosion Science 52, 3654.

Marinca, T.F., Chicinaş, I., Isnard; O., 2012. Influence of the heat treatment conditions on the formationof $CuFe_2O_4$from mechanical milled precursors oxides. Journal of Thermal Analysis and Calorimetry 110, 301.

Rasband, W.S., 2014. “ImageJ”. http://rsb.info.nih.gov/ij/

Special Metals, 2004. *Publication Number SMC-046: INCOLOY® alloy 800*.Special Metals Corporation, Huntington.

Vingsbo, O., S. Söderberg, S., 1988. On fretting maps. Wear 126, 131.

Waterhouse, R.B., 1972.*Fretting Corrosion*.Pergamon Press, Oxford.